Macromolecules

Article

pubs.acs.org/Macromolecules

Sequential "Click" Approach to Polyhedral Oligomeric Silsesquioxane-Based Shape Amphiphiles

Kan Yue,[†] Chang Liu,[†] Kai Guo,[†] Xinfei Yu,[†] Mingjun Huang,[†] Yiwen Li,[†] Chrys Wesdemiotis,[†,‡] Stephen Z. D. Cheng,*[,†] and Wen-Bin Zhang*[,†]

[†]Department of Polymer Science, College of Polymer Science and Polymer Engineering, The University of Akron, Akron, Ohio 44325-3909, United States

[‡]Department of Chemistry, The University of Akron, Akron, Ohio 44325-3601, United States

Supporting Information

ABSTRACT: This paper reports a highly efficient and modular sequential "click" approach for the syntheses of shape amphiphiles based on polymer-tethered polyhedral oligomeric silsesquioxane (POSS). This approach combines both "grafting-to" and "post-functionalization" strategies. It involves the copper-catalyzed Huisgen [3 + 2] cycloaddition (CuAAC) for POSS−polymer ligation and subsequent thiol−ene addition reaction for POSS cage functionalization. Starting from a readily available POSS precursor bearing one alkyne and seven vinyl groups (VPOSS−alkyne), the CuAAC reaction is effective in ensuring the stoichiometric bonding between POSS and azide-functionalized polymers, with no need for fractionation in the purification process. The modularity was demonstrated in two representative polymer systems, hydrophobic polystyrene (PS) and hydrophilic poly(ethylene oxide) (PEO), by the synthesis of VPOSS−PS and VPOSS−PEO. The thiol−ene reaction was subsequently applied to convert all the vinyl groups on the POSS cage quantitatively into various functional groups, including carboxylic acids, hydroxyls, and alkyls, thereby introducing amphiphilicity to drive self-assembly. Such shape amphiphiles are novel model systems for the study of their self-assembly behaviors, hierarchal structure formation, and functional properties in both the solution and bulk states. Aiming to fulfill the "click" philosophy, the sequential "click" approach described here is robust and efficient for rapid construction of functional shape amphiphiles with complex structures and diverse molecular architectures.

INTRODUCTION

Amphiphilic molecules have attracted numerous research interests in academia and have found wide applications in industry.[1−3] Recently, the scope of amphiphiles have been extended beyond traditional small-molecule surfactants and amphiphilic block copolymers,[1] to include amphiphilic dendrimers,[4] modified colloidal particles,[5] supramolecular assemblies,[6] and inorganic−organic hybrids.[7] Besides chemical heterogeneity, symmetry breaking in molecular shapes leads to an even broader concept of shape amphiphiles.[8,9]

Shape amphiphiles are built from building blocks with incompatible packing geometries and distinct interaction parameters.[10−14] Their self-assemblies are driven by competing interactions and shape incommensurateness between subunits and have been predicted to form versatile ordered structures across different length scales.[10−12] The possibility to tune the self-assembly through rational molecular design and precise chemical modification promises the "bottom-up" strategy[15] in the low-cost fabrication of ordered structures with nanometer feature sizes.[16] One representative model shape amphiphile is a shape-persistent nano-object (such as nanospheres[10] and nanorods[12]) tethered with flexible polymer tails. Various ordered phases can be generated by adjusting (1) the interaction parameters between the subunits; (2) the symmetry and size of the nanoparticles; and (3) the length, number, and position of the tethered polymer tails.[12,13] With the rapid development of nanotechnology, a number of nanobuilding blocks are now available, including inorganic nanoparticles,[17] carbon nanotubes,[18] supramolecular nanoclusters,[19] dendrimers,[20] and molecular nanoparticles (MNPs).[21,22] Among these, two MNPs, namely, polyhedral oligomeric silsesquioxanes (POSS) and [60]fullerene (C_{60}), have been used as the major building blocks to prepare shape amphiphiles in our group.[23−32]

The POSS molecules are a family of three-dimensional (3D) cage compounds with silicon−oxygen backbones.[21,33−36] The unique structures and properties have stimulated broad research interests in POSS−polymer hybrids including either physically blending POSS with various polymers[37,38] or chemically incorporating them into polymers.[39−44] Modifications of functional groups on the POSS periphery have been recognized as one effective way to control the physical properties of POSS and to promote the self-assembly of such hybrids.[45,46] Functionalization of POSS can occur either before or after the attachment to polymer tail(s) (i.e., the pre- or post-functionalization approach). The latter is advantageous if multiple-site, simultaneous functionalization can be readily achieved in a single reaction step.

Received: June 26, 2012
Revised: September 19, 2012
Published: October 1, 2012

dx.doi.org/10.1021/ma3013256 | *Macromolecules* 2012, 45, 8126−8134

Scheme 1. General Sequential "Click" Strategy to Functional Materials

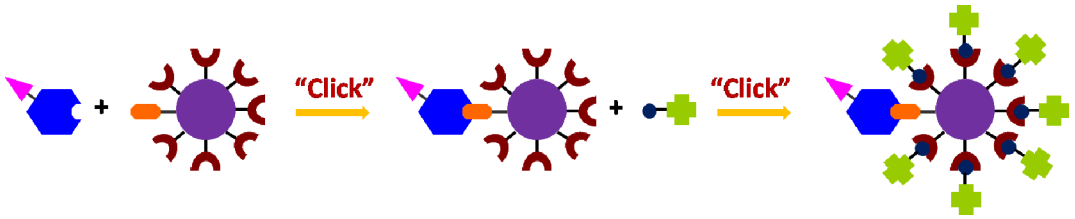

Scheme 2. Sequential "Click" Approach to XPOSS–PS and HexPOSS–PEO[a]

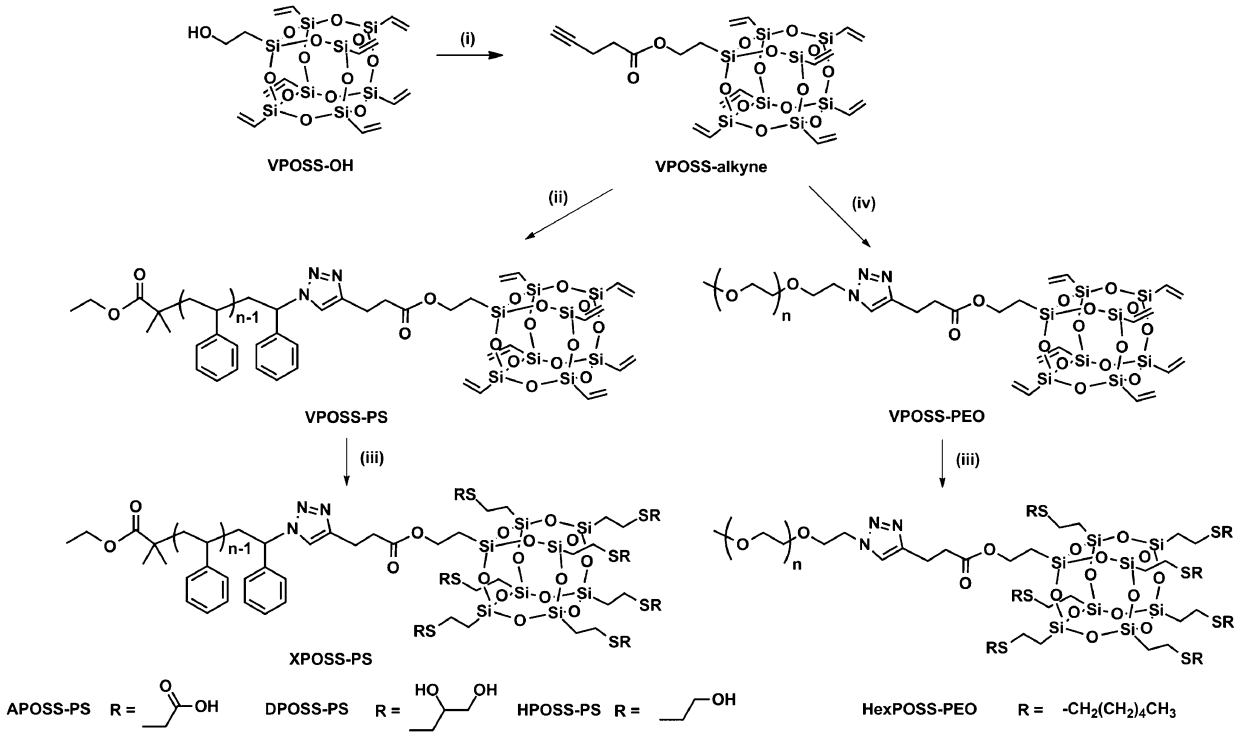

[a](i) 4-Pentynoic acid, DIPC, DMAP, DCM, room temperature, 90%; (ii) PS–N_3 (1.0 equiv), CuBr, PMDETA, toluene, room temperature, 85%; (iii) RSH, Irgacure 2959, THF, *hv*, 15 min, ~70–80%; (iv) PEO–N_3 (0.95 equiv), CuBr, PMDETA, toluene, room temperature, 82%.

Because of the high efficiency and functional group tolerance of the thiol–ene reaction, vinyl-functionalized POSS (VPOSS) can be used as a versatile precursor to POSS with diverse peripheral functional groups (XPOSS).[47−49] The VPOSS–polymer hybrids have been synthesized by both "grafting-to"[29] and "growing-from"[26,32,50] approaches and have been transformed to various XPOSS–polymer hybrids via the thiol–ene reaction. However, they either suffer from byproduct that can only be removed by tedious, repetitive fractionation or are limited by the polymerization methods that are compatible with the VPOSS building block.[26,29] It is desirable to expand the scope of tethered polymer tails to include those of diverse chemical compositions and complex architectures (such as cyclic, dendritic, and hyper-branched polymers). Hence, it calls for a generally applicable and highly efficient synthetic methodology to prepare functionalized POSS–based shape amphiphiles.

Since its debut in 2001, the application of "click" chemistry has become prevalent in chemical science.[51,52] The "click" philosophy is best embodied by synthesizing complex and diverse structures from a library of simple building blocks using a series of "click" reactions—the so-called sequential "click" approach (Scheme 1). The strategy has been applied to prepare biofriendly hydrogels,[53] to immobilize carbohydrates and proteins onto solid surfaces,[54] to orthogonally modify "dual-clickable" Janus nanoparticles,[55] to rapidly construct dendrimers up to the sixth generation in a single day,[56] and to synthesize functional polymers,[57,58] to name a few. These examples have demonstrated the power and efficiency of the sequential "click" approach.

Here, we report the application of this strategy to the syntheses of POSS–based shape amphiphiles in two exemplary systems (Scheme 2): (1) XPOSS–PS with a hydrophilic POSS head and a hydrophobic PS tail; (2) HexPOSS–PEO with a hydrophobic POSS head and a hydrophilic PEO tail. The syntheses are straightforward, modular, and robust, yielding precisely defined model shape amphiphiles that facilitate a further systematic study on their self-assembly, structure–property relationships, and potential technological applications.

EXPERIMENTAL SECTION

Chemicals and Solvents. Toluene (ACS grade, EMD), and styrene (99%, Sigma-Aldrich) were purified as reported previously.[23] Methanol (reagent grade, Fisher Scientific), chloroform (Certified ACS, Fisher Scientific), dichloromethane (DCM, Fisher Scientific), ethyl acetate (Fisher Scientific), tetrahydrofuran (THF, Fisher Scientific), *N,N*-dimethylformamide (DMF, anhydrous 99.8%, Sigma-Aldrich), and

dx.doi.org/10.1021/ma3013256 | *Macromolecules* 2012, 45, 8126–8134

hexanes (Certified ACS, Fisher Scientific) were used as received. 2-Mercaptoacetic acid (≥98%, Sigma-Aldrich) was distilled under reduced pressure before use. 4-Pentynoic acid (98%, Acros Organics), *N*,*N*′-diisopropyl carbodiimide (DIPC, 99%, Acros Organics), 1-hexanethiol (95%, Sigma-Aldrich), 4-dimethylaminopyridine (DMAP, ≥ 99%, Sigma-Aldrich), copper(I) bromide (98%, Acros Organics), *N*,*N*,*N*′,*N*″,*N*″-pentamethyl diethylenetriamine (PMDETA, 99%, Sigma-Aldrich), trifluoromethanesulfonic acid (99%, Acros Organics), 2-hydroxy-4′-(2-hydroxyethoxy)-2-methylpropiophenone (Irgacure 2959, 98%, Sigma-Aldrich), 2-mercaptoethanol (≥99%, Sigma-Aldrich), 1-thioglycerol (≥98%,Fluka), poly(ethylene glycol) methyl ether (PEO−OH, M_n = 2.0 kg/mol, Sigma-Aldrich), and OctaVinyl−POSS (OVPOSS, > 97%, Hybrid Plastics) were used as received. Silica gel (Sorbtech Technologies Inc., 230−400 mesh) was activated by heating to 140 °C for 12 h. Monohydroxyl heptavinyl substituted POSS (VPOSS−OH),[59] azide-end-capped PS[23] (PS−N_3), and PEO[60] (PEO−N_3) were synthesized as reported.

Characterization. All ^{1}H and ^{13}C NMR spectra were obtained in $CDCl_3$ (99.8% D, Sigma-Aldrich) at 30 °C using a Varian NMRS 500 spectrometer equipped with an autosampler. For ^{1}H NMR experiments, the sample concentration was ∼10−20 mg/mL; higher concentrations (∼50−80 mg/mL) were generally desired for ^{13}C NMR measurements. The ^{1}H NMR spectra were referenced to the residual proton impurities in the $CDCl_3$ at δ 7.27 ppm, and ^{13}C NMR spectra were referenced to $^{13}CDCl_3$ at δ 77.00 ppm. For VPOSS−polymer, the integration ratio between the characteristic vinyl peaks on POSS at δ 6.25−5.80 ppm (21 H per VPOSS) and the peaks at δ 7.45−6.35 ppm (aromatic protons in PS) for VPOSS−PS or at 3.84−3.48 ppm for VPOSS−PEO gives the number-average degree of polymerization of the polymer block (DP). The calculated molecular weight ($M_{n,NMR}$) can then be obtained by the summation of $M_{n,polymer}$ (DP × 104.1 g/mol for PS and DP × 44.0 g/mol for PEO), $M_{Initiator}$ (115.2 g/mol for PS and 31.0 g/mol for PEO), and M_{XPOSS} (773.2 g/mol for VPOSS, 1418.0 g/mol for APOSS, 1530.3 g/mol for DPOSS, 1320.1 g/mol for HPOSS, and 1600.9 g/mol for HexPOSS).

Infrared spectra of polymer products were recorded on an Excalibur Series FT-IR spectrometer (DIGILAB, Randolph, MA) by drop-casting sample films on a KBr plate from polymer solutions in THF (∼10 mg/mL), with subsequent drying at room temperature by blowing air. The data were processed using the Win-IR software.

Matrix-assisted laser desorption/ionization time-of-flight (MALDI−TOF) mass spectra were recorded on a Bruker Ultraflex III TOF/TOF mass spectrometer (Bruker Daltonics, Billerica, MA) equipped with a Nd:YAG laser which emits at 355 nm. The matrix used in MALDI-TOF MS measurements was *trans*-2-[3-(4-*tert*-butylphenyl)-2-methyl-2-propenylidene]malononitrile (DCTB, > 99%, Aldrich) and was dissolved in $CHCl_3$ at a concentration of 20.0 mg/mL. Sodium trifluoroacetate (NaTFA) was used as the cationizing agent and was prepared in a MeOH/$CHCl_3$ (v/v = 1/3) solution at a concentration of 10.0 mg/mL. The matrix and cationizing agent solutions were mixed in the ratio of 10/1 (v/v). The sample was prepared by depositing 0.5 μL of matrix and salt mixture on the wells of a 384-well ground-steel plate, allowing the spots to dry, depositing 0.5 μL of each sample on a spot of dry matrix, and adding another 0.5 μL of matrix and salt mixture on top of the dry sample (the sandwich method).[61] Mass spectra were measured in the reflection mode, and the mass scale was calibrated externally with a PMMA standard at the molecular weight region under consideration. Data analyses were conducted with the Bruker's flexAnalysis software.

Size exclusion chromatograms (SEC) were obtained from a Waters 150-C Plus instrument equipped with three HR-Styragel columns [100 Å, mixed bed (50/500/10^3/10^4 Å), mixed bed (10^3, 10^4, 10^6 Å)], and a triple detector system. The three detectors included a differential viscometer (Viscotek 100), a differential refractometer (Waters 410), and a laser light scattering detector (Wyatt Technology, DAWN EOS, λ = 670 nm). The instrument was calibrated with polystyrene standards whose molecular weights range from 580 to 841 000 g/mol. THF was used as the eluent at a flow rate of 1.0 mL/min at 35 °C. The sample solution was prepared in THF with a concentration of ∼5−10 mg/mL depending on polymer molecular weight and was filtered through a 0.45 μm Teflon filter before injection. Data processing was accomplished using the workstation software equipped with the system. Molecular weights from SEC experiments ($M_{n,SEC}$ and $M_{w,SEC}$) and polydispersity indexes (PDIs) were obtained from a working curve from polystyrene standards.

VPOSS−Alkyne. To a 100 mL round-bottomed flask equipped with a magnetic stirring bar were added VPOSS−OH (651 mg, 1.0 mmol), 4-pentynoic acid (118 mg, 1.2 mmol), and DMAP (25 mg, 0.2 mmol), followed by the addition of 10 mL of freshly dried CH_2Cl_2 to fully dissolve all the solids. The flask was capped by a rubber septum, cooled to 0 °C, and stirred at that temperature for 10 min. Then, DIPC (189 mg, 1.5 mmol) was added dropwise via syringe. The mixture was allowed to warm up to room temperature and stirred for another 24 h. After that, the white precipitate was filtered off, and the filtrate was washed with water and brine, dried over Na_2SO_4 and evaporated under vacuum. The residue was purified by flash column chromatography on silica gel with hexanes/CH_2Cl_2 (v/v = 1/1) as the eluent to afford the product as a white powder (660 mg). Yield: 90%. ^{1}H NMR ($CDCl_3$, 500 MHz, ppm): δ 6.16−5.86 (m, 21H, vinyl-H), 4.26 (t, J = 2.5 Hz, 2H, $-OCH_2-$), 2.51 (m, 4H, $-CH_2CH_2-$), 1.97 (t, J = 1.5 Hz, 1H, alkyne−H), 1.22 (t, J = 2.5 Hz, 2H, $-SiCH_2-$). ^{13}C NMR ($CDCl_3$, 125 MHz, ppm): δ 171.6, 137.1, 137.1, 137.0, 128.6, 128.45, 128.5, 82.5, 69.0, 60.9, 33.4, 14.3, 13.1. MS (MALDI−TOF, m/z): calcd. monoisotopic mass for $[M{\cdot}Na]^+$ ($C_{21}H_{30}NaO_{14}Si_8$): 753.0 Da, found 752.8 Da (Figure S1, Supporting Information).

VPOSS−PS. To a 100 mL Schlenk flask equipped with a magnetic stirring bar were added VPOSS−alkyne (100 mg, 0.13 mmol, 1.0 equiv), PS−N_3 (M_n = 2.4 kg/mol, PDI = 1.06, 313 mg, 1.0 equiv), CuBr (1 mg, 0.007 mmol, 0.05 equiv), and freshly distilled toluene (10 mL). The resulting solution was degassed by three freeze−pump−thaw cycles before adding PMDETA (20 mg, 24.1 μL, 1.0 equiv) via pipet. The mixture was further degassed by one cycle and was then stirred at room temperature for 12 h. After the reaction was completed, the solution was directly transferred onto a silica gel column. Toluene was first used as the eluent to fully remove the unreacted starting materials, then a mixture of toluene and ethyl acetate (v/v = 1/1) was used to wash the product off the column. After removing the solvent, the crude product was precipitated into cold MeOH and collected by vacuum filtration once and dried under vacuum to afford VPOSS−PS as a white powder (355 mg). Yield: 85%. ^{1}H NMR ($CDCl_3$, 500 MHz, ppm): δ 7.45−6.35 (m, 115H, aromatic protons of PS), 6.25−5.80 (m, 21H, vinyl groups), 5.10 (m, 1H), 4.20 (m, 2H), 3.60 (m, 2H), 2.95 (m, 2H), 2.65 (m, 4H), 2.40−1.20 (m, 69H), 1.20−0.80 (m, 11H). ^{13}C NMR ($CDCl_3$, 125 MHz, ppm): δ 177.4, 172.6, 145.6−144.9, 137.0, 129.1−125.4, 120.0, 63.0, 60.7, 60.0, 46.0−39.8, 33.7, 30.3, 26.8−24.9, 20.9, 13.9, 13.1 (Figure S2a, Supporting Information). FT-IR (KBr) ν (cm^{-1}): 3061, 3027, 2926, 2852, 1945, 1731, 1602, 1493, 1453, 1123 (Si−O−Si asymmetric stretching), 1069, 1029, 908, 759, 699, 577 (Figure S3b, Supporting Information). MS (MALDI−TOF, m/z): calcd monoisotopic mass for $[20mer{\cdot}Na]^+$ ($C_{187}H_{201}N_3NaO_{16}Si_8$), 2991.3 Da; found, 2991.2 Da. $M_{n,NMR}$ = 3.1 kg/mol. SEC: $M_{n,SEC}$ = 3.1 kg/mol, PDI = 1.03.

VPOSS−PEO. The reaction was performed similarly to that of VPOSS−PS using VPOSS−alkyne (53 mg, 0.072 mmol) and PEO−N_3 (M_n = 2.0 kg/mol, PDI = 1.11, 136 mg, 0.068 mmol, 0.95 equiv). The product was purified by flash column chromatography first with toluene as the eluent to remove excess VPOSS−alkyne and then with THF/methanol mixture (v/v = 3/1) to elute the product. After removing the solvent, the product was redissolved in benzene and freeze-dried to give a white solid (152 mg). Yield: 82%. ^{1}H NMR ($CDCl_3$, 500 MHz, ppm): δ 7.49 (m, 1H, on the triazole ring), 6.25−5.80 (m, 21H, vinyl groups), 4.48 (m, 2H), 4.21 (m, 2H), 3.84−3.48 (m, 180H), 3.35 (m, 3H), 3.00 (m, 2H), 2.69 (m, 2H), 1.18 (m, 2H). ^{13}C NMR ($CDCl_3$, 125 MHz, ppm): δ 172.6, 137.0, 128.5, 71.9, 70.6−70.4, 69.5, 60.7, 59.0, 20.9, 13.1 (Figure S4a, Supporting Information). FT-IR (KBr) ν (cm^{-1}): 3066, 2884, 1735, 1467, 1409, 1360, 1344, 1280, 1147, 1112 (Si−O−Si asymmetric stretching), 1061, 965, 842, 778, 577, 463 (Figure S5b, Supporting Information). MS (MALDI−TOF, m/z): calcd monoisotopic mass for $[40mer{\cdot}Na]^+$ ($C_{104}H_{197}N_3NaO_{55}Si_8$), 2615.1 Da;

found, 2615.4 Da. $M_{n,NMR}$ = 2.7 kg/mol. SEC: $M_{n,SEC}$ = 3.2 kg/mol, PDI = 1.10.

General Procedure for the Thiol−Ene "Click" Reaction. To an open vial without stirring bar were added VPOSS−Polymer (0.048 mmol, 1.0 equiv), the corresponding thiol (10.0 equiv per polymer chain, or 1.4 equiv per vinyl group), the photoinitiator Irgacure 2959 (1 mg, 0.0045 mmol, 0.10 equiv per polymer chain, or 0.014 equiv per vinyl group), and a minimum amount of THF (about 2 mL) to fully dissolve the solids. The reaction was complete after irradiation by 365 nm UV light for 15 min. For XPOSS−PS, the mixture was purified by repeated precipitation from concentrated THF solutions of the crude products into MeOH/water mixture (v/v = 1/1). For HexPOSS−PEO, the crude product was transferred onto a silica gel column and purified by first eluting with chloroform to remove excess thiol and then with THF/methanol mixture (v/v = 3/1) to elute the product.

APOSS−PS. 2-Mercaptoacetic acid (44 mg, 0.48 mmol) and 2 mL of THF were used. The product was collected as a white solid (134 mg, 74%). ^{1}H NMR ($CDCl_3$, 500 MHz, ppm): δ 11.00 (br, 7H, COO*H*), 7.45−6.35 (m, 115H), 5.10 (m, 1H), 4.20 (m, 2H), 3.60 (m, 2H), 3.35 (m, 14H), 2.95 (m, 2H), 2.75 (m, 16H), 2.40−1.20 (m, 69H), 1.20−0.80 (m, 25H). ^{13}C NMR ($CDCl_3$, 125 MHz, ppm): δ 177.4, 175.8, 175.1, 172.9, 146.0−144.8, 128.8−125.5, 121.0, 63.7−63.4, 60.7, 59.9, 48.5−41.6, 40.4−39.8, 33.4, 29.6, 26.4, 26.0−24.9, 20.1, 15.6, 13.8, 12.7, 12.1 (Figure S2b, Supporting Information). FT-IR (KBr) ν (cm^{-1}): 3061, 3026, 2926, 2648, 1945, 1726, 1602, 1493, 1452, 1286, 1124 (Si−O−Si asymmetric stretching), 1029, 909, 759, 734, 699, 542, 473 (Figure S3c, Supporting Information). MS (MALDI−TOF, m/z): calcd monoisotopic mass for [20mer·Na]$^+$ ($C_{201}H_{229}N_3NaO_{30}S_7Si_8$), 3635.3 Da; found, 3635.9 Da. $M_{n,NMR}$ = 3.8 kg/mol. SEC: $M_{n,SEC}$ = 3.7 kg/mol, PDI = 1.03.

DPOSS−PS. 1-Thioglycerol (52 mg, 0.48 mmol) and 2 mL of THF were used. The product was collected as a white solid (130 mg, 70%). ^{1}H NMR ($CDCl_3$, 500 MHz, ppm): δ 7.45−6.35 (m, 115H), 5.10 (m, 1H), 4.75−3.90 (m, 16H), 3.85−3.40 (m, 23H), 2.95 (m, 2H), 2.80−2.40 (m, 30H), 2.40−1.20 (m, 69H), 1.20−0.80 (m, 25H). ^{13}C NMR ($CDCl_3$, 125 MHz, ppm): δ 177.4, 172.9, 146.0−144.9, 129.0−125.3, 120.3, 71.1, 65.2, 60.8, 59.9, 46.4−39.8, 35.2, 33.5, 26.7, 26.0−24.9, 20.7, 13.9, 12.8 (Figure S2c, Supporting Information). FT-IR (KBr) ν (cm^{-1}): 3392 (br), 3082, 3061, 3026, 2925, 2854, 1946, 1728, 1602, 1493, 1452, 1284, 1181, 1126 (Si−O−Si asymmetric stretching), 1069, 1030, 909, 759, 700, 542, 473 (Figure S3d, Supporting Information). MS (MALDI−TOF, m/z): calcd monoisotopic mass for [20mer·Na]$^+$ ($C_{208}H_{257}N_3NaO_{30}S_7Si_8$), 3747.5 Da; found, 3747.8 Da. $M_{n,NMR}$ = 3.9 kg/mol. SEC: $M_{n,SEC}$ = 4.1 kg/mol, PDI = 1.05.

HPOSS−PS. 2-Mercaptoethanol (38 mg, 0.48 mmol) and 2 mL of THF were used. The product was collected as a white solid (139 mg, 79%). ^{1}H NMR ($CDCl_3$, 500 MHz, ppm): δ 7.45−6.35 (m, 115H), 5.10 (m, 1H), 4.20 (m, 2H), 3.75−3.40 (m, 16H), 2.90 (m, 9H), 2.80−2.40 (m, 30H), 2.40−1.20 (m, 69H), 1.20−0.80 (m, 25H). ^{13}C NMR ($CDCl_3$, 125 MHz, ppm): δ 177.4, 172.8, 146.0−144.9, 129.0−125.3, 120.3, 60.9, 59.9, 46.4−39.8, 34.9, 33.5, 29.7, 26.0−25.7, 22.6, 13.9, 13.0 (Figure S2d, Supporting Information). FT-IR (KBr) ν (cm^{-1}): 3640, 3397 (br), 3082, 3061, 3027, 2925, 2871, 1945, 1729, 1601, 1493, 1452, 1363, 1281, 1181, 1122 (Si−O−Si asymmetric stretching), 1067, 908, 759, 699, 542, 472 (Figure S3e, Supporting Information). MS (MALDI−TOF, m/z): calcd monoisotopic mass for [20mer·Na]$^+$ ($C_{201}H_{243}N_3NaO_{23}S_7Si_8$), 3537.4 Da; found, 3537.7 Da. $M_{n,NMR}$ = 3.7 kg/mol. SEC: $M_{n,SEC}$ = 3.7 kg/mol, PDI = 1.04.

HexPOSS−PEO. VPOSS−PEO (100 mg, 0.037 mmol), 1-hexanethiol (44 mg, 0.37 mmol), and 2 mL of THF were used. The product was purified by flash column chromatography first with THF as the eluent to remove excess photoinitiator and thiols, and then with THF/methanol mixture (v/v = 3/1) to elute the product. After removing the solvent, the product was redissolved in benzene and freeze-dried to give a white solid (98 mg, 75%). ^{1}H NMR ($CDCl_3$, 500 MHz, ppm): δ 7.49 (m, 1H, on the triazole ring), 4.48 (m, 2H), 4.17 (m, 2H), 3.86−2.48 (m, 180H), 3.36 (m, 3H), 3.01 (m, 2H), 2.70 (m, 2H), 2.58 (m, 14H), 2.50 (m, 14H), 1.56 (m, 14H), 1.37−1.24 (m, 42H), 1.14 (m, 2H), 1.03−0.99 (m, 14H), 0.88 (m, 21H). ^{13}C NMR ($CDCl_3$, 125 MHz, ppm): δ 172.5, 122.1, 71.9, 70.7−70.3, 69.5, 68.1, 64.8, 58.9, 52.4, 51.7, 50.1, 34.8, 33.6, 32.0, 31.4, 28.6, 25.9, 25.5, 22.5, 22.3, 20.9, 14.0, 13.0 (Figure S4b, Supporting Information). FT-IR (KBr) ν (cm^{-1}): 2924, 2866, 1733, 1601, 1557, 1460, 1349, 1282, 1252, 1115 (Si−O−Si asymmetric stretching), 1043, 949, 847, 801 (Figure S5c, Supporting Information). MS (MALDI−TOF, m/z): calcd monoisotopic mass for [40mer·Na]$^+$ ($C_{146}H_{295}N_3NaO_{55}S_7Si_8$), 3441.7 Da; found, 3442.0 Da. $M_{n,NMR}$ = 3.6 kg/mol. SEC: $M_{n,SEC}$ = 3.7 kg/mol, PDI = 1.12.

RESULTS AND DISCUSSION

VPOSS−Alkyne: A "Clickable" XPOSS Precursor. "Click" reactions refer to those highly efficient, modular, regio- and stereospecific reactions that require minimum setup and work-up procedure and yield a single product with minimum by-products.[51] Two reactions, namely, the copper-catalyzed azide−alkyne [3 + 2] cycloaddition (CuAAC)[51,52] reaction and the thiol−ene addition reaction,[47] have been shown to possess most of the features desired for "click" chemistry and have been widely examined and applied, especially in the area of macromolecular modification, where reactivity and reaction efficiency are long-standing problems. Despite the apparently different reactivity between alkyne and alkene, these two reactions are not orthogonal: Thiols would also react with alkynes (the thiol−yne reaction).[62,63] As a result, the CuAAC reaction should be performed prior to thiol−ene functionalization, as shown in Scheme 2. Although the CuAAC "click" reaction has been successfully used to chemically link alkyl-substituted POSS to various polymers,[64] there have been few reports on the use of this reaction to link either VPOSS or XPOSS to other building blocks. Our previous work has demonstrated that VPOSS is a versatile precursor to XPOSS.[26,29] Therefore, a "clickable" VPOSS derivative is highly desirable to fulfill the sequential "click" synthesis of POSS-based shape amphiphiles.

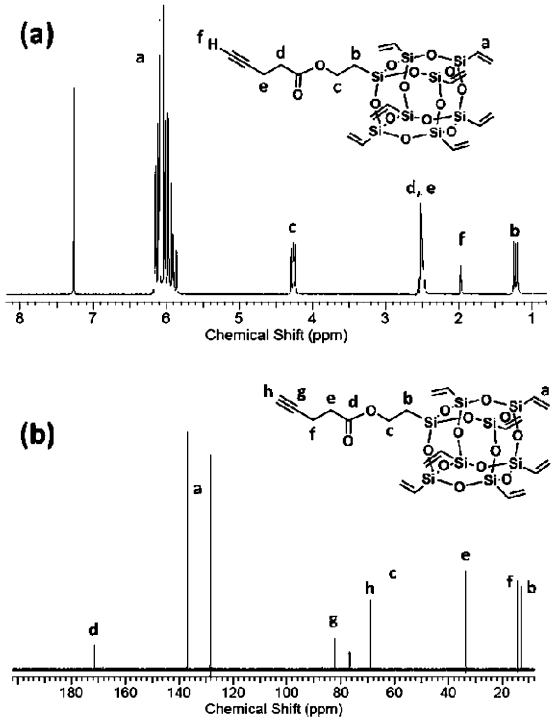

Figure 1. ^{1}H NMR (a) and ^{13}C NMR (b) spectra of VPOSS−alkyne.

dx.doi.org/10.1021/ma3013256 | *Macromolecules* 2012, 45, 8126−8134

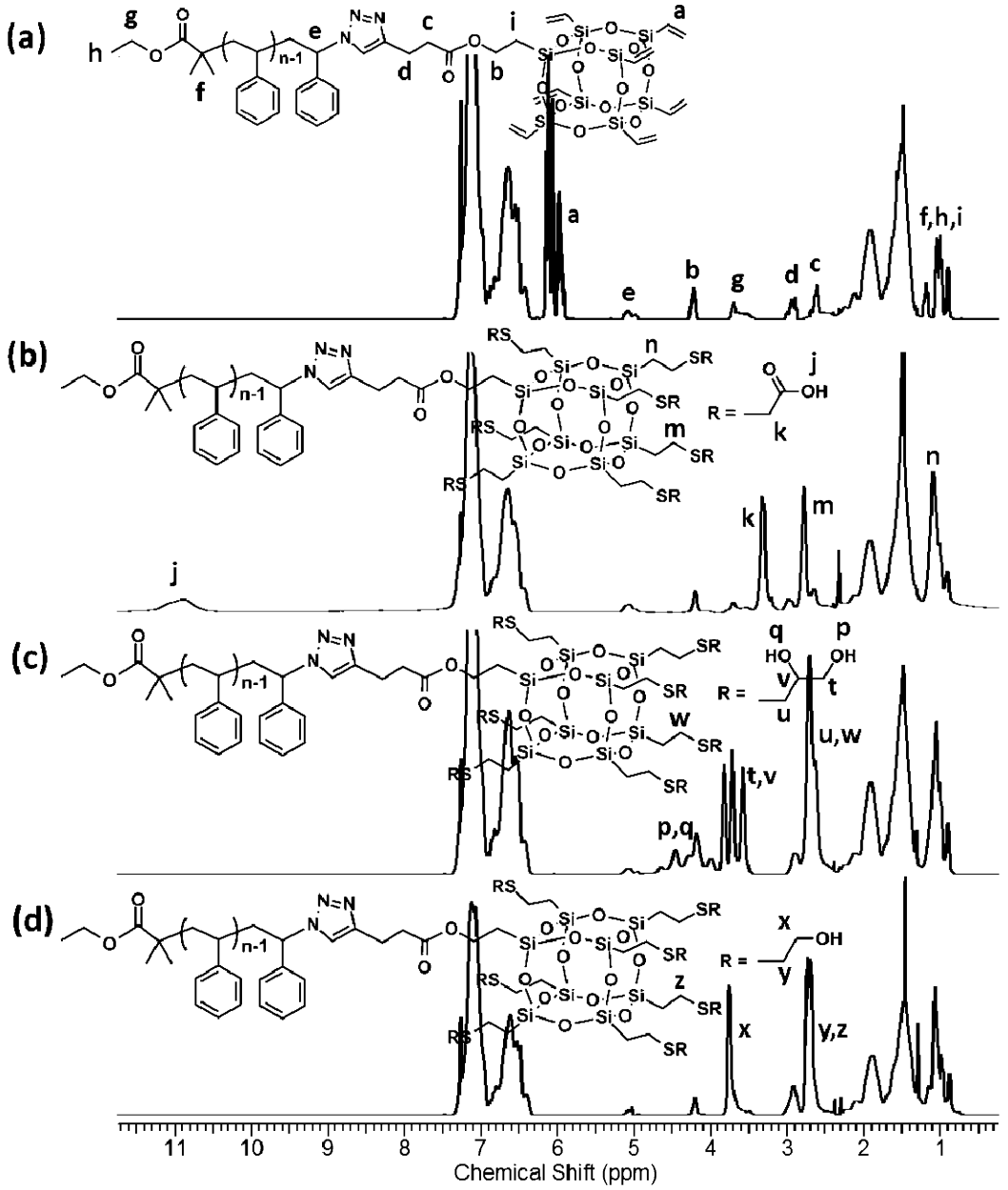

Figure 2. ^{1}H NMR spectra of (a) VPOSS−PS, (b) APOSS−PS, (c) DPOSS−PS, and (d) HPOSS−PS.

Considering the readily available azide-end-capped polymers (PS−N_3, PEO−N_3 etc.), VPOSS−alkyne (Scheme 2) is designed and synthesized by esterification of monohydroxyl vinyl POSS (VPOSS−OH) with 4-pentynoic acid. Promoted by DIPC and DMAP, the Steglich esterification works efficiently at room temperature to afford VPOSS−alkyne in a very good yield (90%). The VPOSS−alkyne is a white powder and has been fully characterized by ^{1}H NMR (Figure 1a), ^{13}C NMR (Figure 1b), and MALDI−TOF mass spectrometry (Figure S1, Supporting Information). The introduction of alkyne is evident by the appearance of a new peak at ∼1.97 ppm for the alkyne proton in the ^{1}H NMR spectrum and two peaks at 82.5 and 69.0 ppm for the alkyne carbons in the ^{13}C NMR spectrum. In addition, the observed m/z value (752.8 Da) in MALDI−TOF mass spectrum (Figure S1, Supporting Information) agrees well with the calculated molecular weight of the product (753.0 Da). These results demonstrate the successful esterification, and the high purity of VPOSS−alkyne is clearly supported by the NMR spectra. The universality of the "clickable" VPOSS−alkyne is subsequently tested in two polymer systems: hydrophobic PS or hydrophilic PEO (Scheme 2).

Model Sequential "Click" Syntheses of XPOSS−PS. The feasibility and efficiency of the sequential "click" approach are first evaluated by using azide-functionalized PS (PS−N_3, M_n = 2.4 kg/mol, PDI = 1.06). Under typical conditions for the CuAAC reaction (CuBr and PMDETA as the catalyst, toluene as the solvent), the cycloaddition proceeds smoothly at room temperature to form the triazole linkage. Purification is conveniently achieved by flash column chromatography on silica gel. The column is eluted first with toluene to remove the excess VPOSS−alkyne or PS−N_3, and then with a mixture of toluene and ethyl acetate to afford VPOSS−PS. After repeated precipitation from a concentrated THF solution into methanol, VPOSS−PS is obtained as a white powder in a good yield (∼85%).

dx.doi.org/10.1021/ma3013256 | *Macromolecules* 2012, 45, 8126−8134

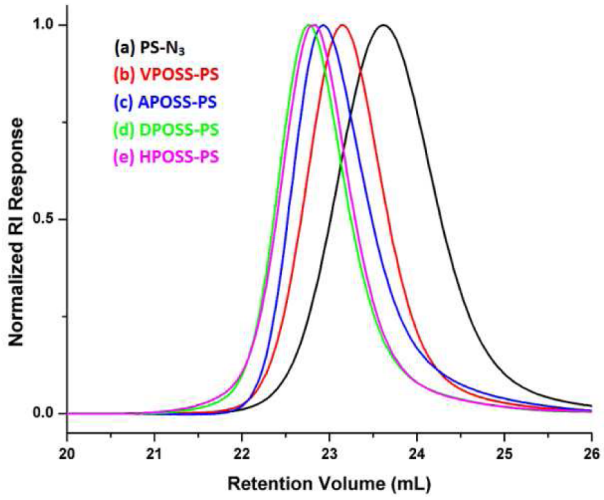

Figure 3. SEC overlay of (a) PS−N_3 (black curve), (b) VPOSS−PS (red curve), (c) APOSS−PS (blue curve), (d) DPOSS−PS (green curve), and (e) HPOSS−PS (pink curve).

The VPOSS−PS is fully characterized by ^{1}H NMR, ^{13}C NMR, FT-IR, and SEC techniques, as well as MALDI−TOF mass spectrometry. In the FT-IR spectrum, the strong azide band at ∼2100 cm^{-1} fully disappears (Figure S3b, Supporting Information), indicating the complete consumption of the azide. The strong band at ∼1123 cm^{-1} is attributed to the asymmetric stretching of Si−O−Si backbone of the POSS cage. The presence of the VPOSS cage is also proven by the signals from the vinyl protons on the POSS cage at 6.25−5.80 ppm (proton **a** in Figure 2a). The integration ratio between the aromatic proton peak area from the PS tail and that from the vinyl groups is about 5.5, which is in good agreement with the calculated value based on the starting material PS−N_3 (M_n = 2.4 kg/mol, DP_n = 23, 115H/21*H* = 5.5). The vinyl sp^2 carbons can also be observed clearly in the ^{13}C NMR spectrum (Figure S2a, Supporting Information) at 137.0 and 128.5 ppm, respectively, where the latter is overlapped with those of the aromatic sp^2 carbons of PS. Proton **e** in Figure 2a appears at ∼5.10 ppm, which is characteristic of the triazole end-capped PS chains.[65,66] However, the proton on the newly formed triazole ring cannot be distinguished. It is speculated that it might overlap with the peaks of the aromatic protons of PS. A model reaction is then conducted between benzyl azide and VPOSS−alkyne (see Supporting Information for details). Indeed, the ^{1}H NMR spectrum of the model compound (Benzyl-VPOSS, see Scheme S1, Supporting Information) clearly shows that the chemical shift of the proton on the triazole ring is ∼7.40 ppm and overlaps with that of the aromatic protons of the benzyl group (see Figure S6, Supporting Information).

Moreover, the SEC overlay (Figure 3) reveals a decreased retention volume of VPOSS−PS relative to PS−N_3, which is consistent with the increased molecular weight of VPOSS−PS (M_n = 3.1 kg/mol) and a larger hydrodynamic volume. The PDI remains narrow (PDI = 1.03), suggesting high uniformity of the product. The most striking evidence comes from the MALDI−TOF mass spectrum as shown in Figure 4a. Only one single symmetric distribution of molecular weights is observed, where the monoisotopic mass of each peak matches well with that expected for the proposed structure (e.g., for $[20mer{\cdot}Na]^+$, found 2991.2 Da vs calcd. 2991.3 Da). The difference between neighboring peaks equals the mass of a styrene repeating unit (104.1 Da). These data unambiguously confirm the precisely defined structure and the molecular homogeneity of the first "clicked" product VPOSS−PS.

Our group has demonstrated that the thiol−ene "click" reaction is an efficient method to quantitatively convert all the vinyl groups on the POSS cages into various functional groups. It

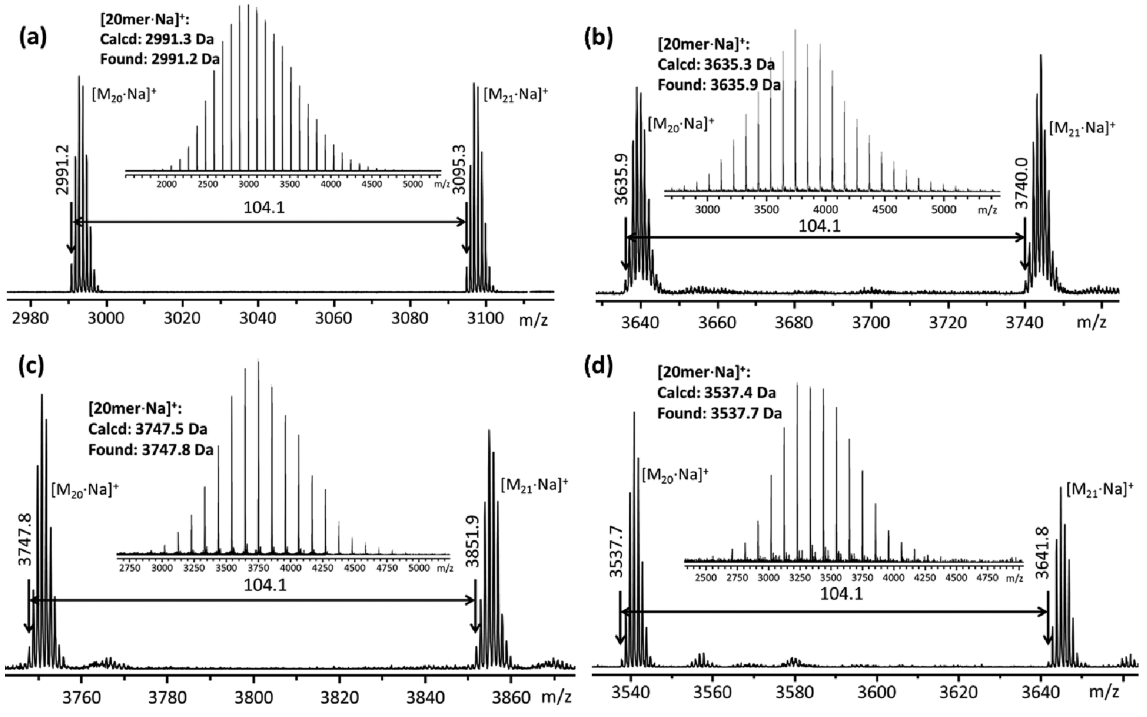

Figure 4. MALDI−TOF mass spectra of (a) VPOSS−PS, (b) APOSS−PS, (c) DPOSS−PS, and (d) HPOSS−PS. All these data were acquired with monoisotopic resolution. The insets show the full spectrum.

dx.doi.org/10.1021/ma3013256 | *Macromolecules* 2012, 45, 8126−8134

Table 1. Summary of Molecular Characterizations of XPOSS−PS and XPOSS−PEO Polymers

sample	molecular formula	M_{Calcd} (Da)	M_{Found} (Da)	$M_{n,NMR}$ [c] (kg/mol)	$M_{n,SEC}$ [d] (kg/mol)	$M_{w,SEC}$ [d] (kg/mol)	PDI[d]
VPOSS−PS	$C_{187}H_{201}N_3NaO_{16}Si_8$ [a]	2991.3[a]	2991.2[a]	3.1	3.1	3.2	1.03
APOSS−PS	$C_{201}H_{229}N_3NaO_{30}S_7Si_8$ [a]	3635.3[a]	3635.9[a]	3.8	3.7	3.8	1.03
DPOSS−PS	$C_{208}H_{257}N_3NaO_{30}S_7Si_8$ [a]	3747.5[a]	3747.8[a]	3.9	4.1	4.3	1.05
HPOSS−PS	$C_{201}H_{243}N_3NaO_{23}S_7Si_8$ [a]	3537.4[a]	3537.7[a]	3.7	3.8	4.0	1.04
VPOSS−PEO	$C_{104}H_{197}N_3NaO_{55}Si_8$ [b]	2615.1[b]	2615.4[b]	2.7	3.2	3.5	1.10
HexPOSS−PEO	$C_{146}H_{295}N_3NaO_{55}S_7Si_8$ [b]	3341.7[b]	3342.0[b]	3.6	3.7	4.1	1.12

[a]These data are based on 20mer with a sodium ion ($[20mer{\cdot}Na]^+$). [b]These data are based on 40mer with a sodium ion ($[40mer{\cdot}Na]^+$). [c]These data are calculated based on ^{1}H NMR spectra. [d]These data are obtained from SEC measurements.

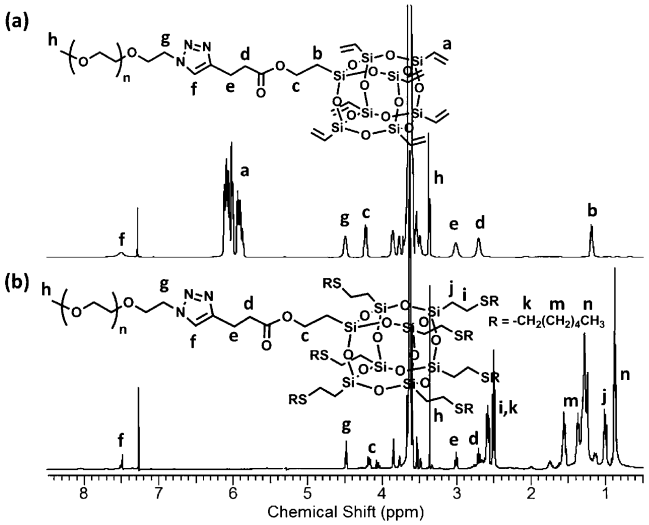

Figure 5. ^{1}H NMR spectra of (a) VPOSS−PEO and (b) HexPOSS−PEO.

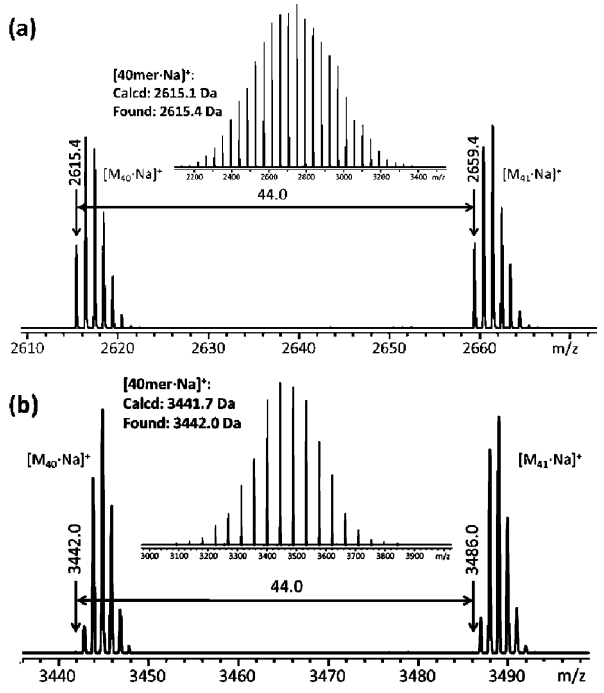

Figure 6. MALDI−TOF mass spectra of (a) VPOSS−PEO and (b) HexPOSS−PEO. All these data are acquired with monoisotopic resolution. The insets show the full spectrum.

is thus used here to afford various model shape amphiphiles. The reactions are performed under similar reaction conditions as

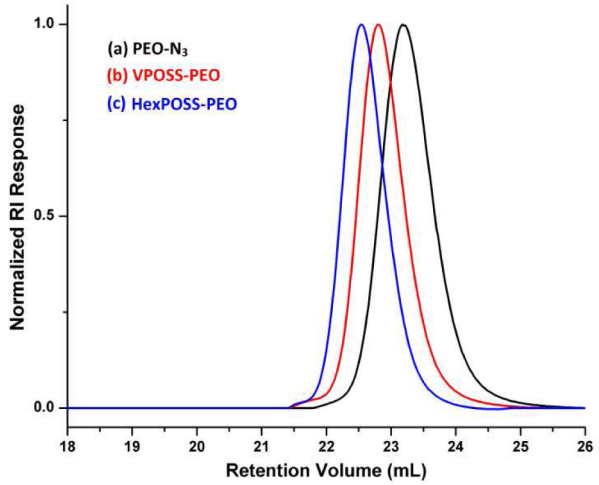

Figure 7. SEC overlay of (a) PEO−N_3 (black curve), (b) VPOSS−PEO (red curve), and (c) HexPOSS−PEO (blue curve).

reported previously,[26] except that a water-soluble photoinitiator Irgacure 2959 is used. Its use facilitates the purification by repeated precipitation into a MeOH/water mixture to fully remove the excess initiator as well as the thiols. After 15 min of UV irradiation, the reaction reaches complete conversion based on the ^{1}H NMR spectrum where the vinyl resonance peaks at 6.25−5.80 ppm fully disappear. The emergence of new resonance peaks is in correspondence to the formation of the thiol ether linkages, confirming the success of the thiol−ene addition reactions. As shown in Figure 2, all of the newly introduced functional groups can be detected and unambiguously assigned. The complete reactions are further supported by the disappearance of the resonance peak at ∼137.0 ppm in the ^{13}C NMR spectra (Figure S2b−S2d, Supporting Information).

From the SEC overlay shown in Figure 3, it is evident that the SEC traces of the products all shifted to smaller retention volumes after the thiol−ene reactions due to the increased molecular weights. Although the difference in molecular weight between DPOSS−PS and HPOSS−PS is small (∼210 Da), there is still a distinguishable shift in peak position. The difference in peak position of APOSS−PS relative to VPOSS−PS is not as much as that of HPOSS−PS, although APOSS−PS has a slightly higher average molecular weight than HPOSS−PS. It is speculated that the carboxylic acid groups of the APOSS−PS may have stronger intramolecular hydrogen bonds, resulting in a more compact hydrodynamic volume in THF solution and a larger retention volume. The structural homogeneity of these shape amphiphiles is also examined by MALDI−TOF mass spectrometry. In Figure 4b−d, all of the spectra show a major distribution and the observed monoisotopic mass values for each peak are in excellent agreement with the calculated ones, as

dx.doi.org/10.1021/ma3013256 | Macromolecules 2012, 45, 8126−8134

summarized in Table 1. The diversification of the peripheral functional groups on the POSS cage is, therefore, successful.

Extending the Strategy to the PEO System. The sequential "click" approach is further applied to the PEO system. Although POSS−PEO hybrids have been prepared by the hydrosilylation reaction and the isocyanate-hydroxyl condensation with over 95% functionalization,[67−69] quantitative functionalization and versatile peripheral group control have not been demonstrated. Our sequential "click" approach is notably advantageous in that the POSS cage is unstable under the basic conditions usually used for the ring-opening polymerization of ethylene oxide.

Because of the high polarity of PEO, a slightly excess amount of VPOSS−alkyne is used to fully consume PEO−N_3 to facilitate purification by flash chromatography on silica gel. The reaction is monitored by FT-IR spectroscopy (Figure S5, Supporting Information). After the reaction is complete, removal of the excess VPOSS−alkyne is achieved by flash column chromatography on silica gel with toluene as the eluent, and the desired product is further eluted with a THF/MeOH mixture (v/v = 3/1). Because of PEO's low molecular weight, precipitation into ethyl ether or hexane gives very low yields. Alternatively, the eluted product is redissolved in benzene, and freeze-dried to give VPOSS−PEO as a white powder. The precisely defined structure of the VPOSS−PEO is confirmed by ^{1}H NMR (Figure 5a), ^{13}C NMR (Figure S4, Supporting Information), and MALDI−TOF mass spectrometry (Figure 6a).

A low-molecular-weight hydrophobic thiol (1-henxanethiol) is subsequently used to functionalize the POSS cage. After the thiol−ene reaction, the purification is achieved by flash column chromatography on silica gel followed by freeze-drying from a benzene solution. This new compound is characterized by all of the routine techniques to prove its precisely defined structure. The quantitative multisite functionalization is evidenced not only by the complete disappearance of vinyl protons at ∼6.0 ppm in the ^{1}H NMR spectrum (Figure 5b) and vinyl sp^2 carbons at 137.0 and 128.5 ppm in the ^{13}C NMR spectrum (Figure S4b, Supporting Information), but also by a single molecular weight distribution in the MALDI−TOF mass spectrum (Figure 6b) and a clear shift of the retention volume in the SEC overlay (Figure 7). The molecular characterizations are also summarized in Table 1. The generality and effectiveness of the sequential "click" approach have thus been established.

It is anticipated that this approach should be equally applicable to polymers of other compositions and architectures with azide functionality, leading to a large variety of shape amphiphiles. In fact, this approach has been utilized in our group for synthesizing a multitude of POSS-based shape amphiphiles that are difficult to synthesize using other methods. Those results will be discussed in future publications. Although only gram-scale synthesis has been demonstrated in this paper, the reactions should be friendly to scaling up owing to the feature of "click" chemistry.[51] It is also worth mentioning that VPOSS−alkyne has been synthesized on the 20 g scale in our laboratory, which can give hundreds of grams of VPOSS−polymer hybrids upon conjugation. The results demonstrate the robustness and versatility of the sequential "click" approach in synthesizing POSS-based shape amphiphiles.

CONCLUSION

In summary, we have developed a sequential "click" approach as a general, modular, and efficient methodology for the syntheses of novel shape amphiphiles based on functionalized XPOSS. The synthetic route features the combination of two consecutive "click" reactions: The copper-catalyzed Huisgen [3 + 2] cycloaddition for "grafting" the VPOSS to polymers and the thiol−ene reaction for the multiple-site simultaneous functionalization on the POSS cages. The tethered entities can be changed in the first "click" reaction, as demonstrated by the two examples in this paper, a hydrophobic PS and a hydrophilic PEO. It is expected that not only polymers of distinct chain topology, but also of unique chemical composition can be synthesized similarly. The functional groups on the POSS periphery are introduced in the second "click" reaction, achieving various XPOSS−Polymer shape amphiphiles from a common precursor VPOSS−Polymer. Using the current approach, one can tether one or more XPOSS cages to essentially any functional materials of complex structures and unique composition provided that their functional groups are compatible with the two "click" reactions. It allows a systematic tuning of the molecular parameters of shape amphiphiles to elucidate the structure−property relationships and to explore those exotic hybrids that are intriguing in their own merit. Work is ongoing in our laboratory to further extend the scope of the MNP-based shape amphiphiles and to reveal underlying physical principles responsible for their unique self-assembly behavior and hierarchical structure formation, both in solution and in the bulk state.

ASSOCIATED CONTENT

Supporting Information

Additional characterization data such as MALDI−TOF mass spectra data for VPOSS−alkyne, ^{13}C NMR spectra and FT-IR spectra of the polymer products summarized in Table 1. The experimental details, results and discussions of the control experiment are also provided. This material is available free of charge via the Internet at http://pubs.acs.org.

AUTHOR INFORMATION

Corresponding Author

*E-mail: (W.-B.Z.) wz8@uakron.edu; (S.Z.D.C.) scheng@uakron.edu.

Notes

The authors declare no competing financial interest.

ACKNOWLEDGMENTS

This work is supported by NSF (DMR-0906898) and the Joint-Hope Foundation.

REFERENCES

(1) Holmberg, K.; Jönsson, B.; Kronberg, B.; Lindman, B. *Surfactants and Polymers in Aqueous Solution*, 2nd ed.; John Wiley & Sons Ltd.: Oxford, England, 2003.
(2) Zhang, L.; Eisenberg, A. *Science* **1995**, *268*, 1728−1731.
(3) Zhang, L.; Eisenberg, A. *J. Am. Chem. Soc.* **1996**, *118*, 3168−3181.
(4) Percec, V.; Wilson, D. A.; Leowanawat, P.; Wilson, C. J.; Hughes, A. D.; Kaucher, M. S.; Hammer, D. A.; Levine, D. H.; Kim, A. J.; Bates, F. S.; Davis, K. P.; Lodge, T. P.; Klein, M. L.; DeVane, R. H.; Aqad, E.; Rosen, B. M.; Argintaru, A. O.; Sienkowska, M. J.; Rissanen, K.; Nummelin, S.; Ropponen, J. *Science* **2010**, *328*, 1009−1014.
(5) Chen, Q.; Bae, S. C.; Granick, S. *Nature* **2011**, *469*, 381−384.
(6) Zhang, X.; Wang, C. *Chem. Soc. Rev.* **2011**, *40*, 94−101.
(7) Park, S.; Lim, J.-H.; Chung, S.-W.; Mirkin, C. A. *Science* **2004**, *303*, 348−351.
(8) Date, R. W.; Bruce, D. W. *J. Am. Chem. Soc.* **2003**, *125*, 9012−9013.
(9) Glotzer, S. C. *Science* **2004**, *306*, 419−420.
(10) Zhang, Z. L.; Horsch, M. A.; Lamm, M. H.; Glotzer, S. C. *Nano Lett.* **2003**, *3*, 1341−1346.

(11) Glotzer, S. C.; Horsch, M. A.; Iacovella, C. R.; Zhang, Z.; Chan, E. R.; Zhang, X. *Curr. Opin. Colloid Interface Sci.* **2005**, *10*, 287−295.
(12) Horsch, M. A.; Zhang, Z.; Glotzer, S. C. *Phys. Rev. Lett.* **2005**, *95*, 056105.
(13) Iacovella, C. R.; Horsch, M. A.; Zhang, Z.; Glotzer, S. C. *Langmuir* **2005**, *21*, 9488−9494.
(14) Glotzer, S. C.; Solomon, M. J. *Nat. Mater.* **2007**, *6*, 557−562.
(15) Whitesides, G. M.; Grzybowski, B. *Science* **2002**, *295*, 2418−2421.
(16) Tang, C.; Lennon, E. M.; Fredrickson, G. H.; Kramer, E. J.; Hawker, C. J. *Science* **2008**, *322*, 429−432.
(17) Xia, Y.; Xiong, Y.; Lim, B.; Skrabalak, S. E. *Angew. Chem., Int. Ed.* **2009**, *48*, 60−103.
(18) Baughman, R. H.; Zakhidov, A. A.; de Heer, W. A. *Science* **2002**, *297*, 787−792.
(19) Fujita, M.; Tominaga, M.; Hori, A.; Therrien, B. *Acc. Chem. Res.* **2005**, *38*, 369−378.
(20) Newkome, G. R.; Moorefield, C. N.; Vögtle, F. *Dendritic Macromolecules: Concepts, Syntheses, Perspectives*; Wiley-VCH: New York, 1997.
(21) Cordes, D.; Lickiss, P.; Rataboul, F. *Chem. Rev.* **2010**, *110*, 2081−2254.
(22) Prassides, K.; Alloul, H. *Fullerene-Based Materials: Structures and Properties*; Springer: Berlin and New York, 2004.
(23) Zhang, W.-B.; Tu, Y.; Ranjan, R.; Van Horn, R. M.; Leng, S.; Wang, J.; Polce, M. J.; Wesdemiotis, C.; Quirk, R. P.; Newkome, G. R.; Cheng, S. Z. D. *Macromolecules* **2008**, *41*, 515−517.
(24) Ren, X.; Sun, B.; Tsai, C.-C.; Tu, Y.; Leng, S.; Li, K.; Kang, Z.; Horn, R. M. V.; Li, X.; Zhu, M.; Wesdemiotis, C.; Zhang, W.-B.; Cheng, S. Z. D. *J. Phys. Chem. B* **2010**, *114*, 4802−4810.
(25) Zhang, W.-B.; Sun, B.; Li, H.; Ren, X.; Janoski, J.; Sahoo, S.; Dabney, D. E.; Wesdemiotis, C.; Quirk, R. P.; Cheng, S. Z. D. *Macromolecules* **2009**, *42*, 7258−7262.
(26) Zhang, W.-B.; Li, Y.; Li, X.; Dong, X.; Yu, X.; Wang, C.-L.; Wesdemiotis, C.; Quirk, R. P.; Cheng, S. Z. D. *Macromolecules* **2011**, 2589−2596.
(27) Zhang, W.-B.; He, J.; Dong, X.; Wang, C.-L.; Li, H.; Teng, F.; Li, X.; Wesdemiotis, C.; Quirk, R. P.; Cheng, S. Z. D. *Polymer* **2011**, *52*, 4221−4226.
(28) Dong, X.-H.; Zhang, W.-B.; Li, Y.; Huang, M.; Zhang, S.; Quirk, R. P.; Cheng, S. Z. D. *Polym. Chem.* **2012**, *3*, 124−134.
(29) Yu, X.; Zhong, S.; Li, X.; Tu, Y.; Yang, S.; Van Horn, R. M.; Ni, C.; Pochan, D. J.; Quirk, R. P.; Wesdemiotis, C.; Zhang, W.-B.; Cheng, S. Z. D. *J. Am. Chem. Soc.* **2010**, *132*, 16741−16744.
(30) Li, Y.; Zhang, W.-B.; Hsieh, I. F.; Zhang, G.; Cao, Y.; Li, X.; Wesdemiotis, C.; Lotz, B.; Xiong, H.; Cheng, S. Z. D. *J. Am. Chem. Soc.* **2011**, *133*, 10712−10715.
(31) Yu, X.; Zhang, W.-B.; Yue, K.; Li, X.; Liu, H.; Xin, Y.; Wang, C.-L.; Wesdemiotis, C.; Cheng, S. Z. D. *J. Am. Chem. Soc.* **2012**, *134*, 7780−7787.
(32) He, J.; Yue, K.; Liu, Y.; Yu, X.; Ni, P.; Cavicchi, K. A.; Quirk, R. P.; Chen, E.-Q.; Cheng, S. Z. D.; Zhang, W.-B. *Polym. Chem.* **2012**, *3*, 2112−2120.
(33) Voronkov, M.; Lavrent'yev, V. *Top. Curr. Chem.* **1982**, *102*, 199−236.
(34) Baney, R. H.; Itoh, M.; Sakakibara, A.; Suzuki, T. *Chem. Rev.* **1995**, *95*, 1409−1430.
(35) Loy, D. A.; Shea, K. J. *Chem. Rev.* **1995**, *95*, 1431−1442.
(36) Laine, R. M. *J. Mater. Chem.* **2005**, *15*, 3725−3744.
(37) Kuo, S.-W.; Chang, F.-C. *Prog. Polym. Sci.* **2011**, *36*, 1649−1696.
(38) Kannan, R. Y.; Salacinski, H. J.; Butler, P. E.; Seifalian, A. M. *Acc. Chem. Res.* **2005**, *38*, 879−884.
(39) Cardoen, G.; Coughlin, E. B. *Macromolecules* **2004**, *37*, 5123−5126.
(40) Goffin, A.-L.; Duquesne, E.; Moins, S.; Alexandre, M.; Dubois, P. *Eur. Polym. J.* **2007**, *43*, 4103−4113.
(41) Zhang, W.; Fang, B.; Walther, A.; Müller, A. H. E. *Macromolecules* **2009**, *42*, 2563−2569.
(42) Li, G.; Wang, L.; Ni, H.; Pittman, C. U. *J. Inorg. Organomet. Polym.* **2001**, *11*, 123−154.
(43) Phillips, S. H.; Haddad, T. S.; Tomczak, S. J. *Curr. Opin. Solid State Mater. Sci.* **2004**, *8*, 21−29.
(44) Wu, J.; Mather, P. T. *Polym. Rev.* **2009**, *49*, 25−63.
(45) Tanaka, K.; Ishiguro, F.; Chujo, Y. *J. Am. Chem. Soc.* **2010**, *132*, 17649−17651.
(46) Mabry, J.; Vij, A.; Iacono, S.; Viers, B. *Angew. Chem., Int. Ed.* **2008**, *47*, 4137−4177.
(47) Hoyle, C. E.; Bowman, C. N. *Angew. Chem., Int. Ed.* **2010**, *49*, 1540−1573.
(48) Kade, M. J.; Burke, D. J.; Hawker, C. J. *J. Polym. Sci., Part A: Polym. Chem.* **2010**, *48*, 743−750.
(49) van der Ende, A. E.; Harrell, J.; Sathiyakumar, V.; Meschievitz, M.; Katz, J.; Adcock, K.; Harth, E. *Macromolecules* **2010**, *43*, 5665−5671.
(50) Li, Y.; Dong, X.-H.; Guo, K.; Wang, Z.; Chen, Z.; Wesdemiotis, C.; Quirk, R. P.; Zhang, W.-B.; Cheng, S. Z. D. *ACS Macro Lett.* **2012**, *1*, 834−839.
(51) Kolb, H. C.; Finn, M. G.; Sharpless, K. B. *Angew. Chem., Int. Ed.* **2001**, *40*, 2004−2021.
(52) Iha, R. K.; Wooley, K. L.; Nystrom, A. M.; Burke, D. J.; Kade, M. J.; Hawker, C. J. *Chem. Rev.* **2009**, *109*, 5620−5686.
(53) DeForest, C. A.; Polizzotti, B. D.; Anseth, K. S. *Nat. Mater.* **2009**, *8*, 659−664.
(54) Sun, X.-L.; Stabler, C. L.; Cazalis, C. S.; Chaikof, E. L. *Bioconjugate Chem.* **2005**, *17*, 52−57.
(55) Zhang, S.; Li, Z.; Samarajeewa, S.; Sun, G.; Yang, C.; Wooley, K. L. *J. Am. Chem. Soc.* **2011**, *133*, 11046−11049.
(56) Antoni, P.; Robb, M. J.; Campos, L.; Montanez, M.; Hult, A.; Malmström, E.; Malkoch, M.; Hawker, C. J. *Macromolecules* **2010**, *43*, 6625−6631.
(57) Yuan, Y.-Y.; Du, J.-Z.; Wang, J. *Chem. Commun.* **2012**, *48*, 570−572.
(58) Zhang, S.; Li, A.; Zou, J.; Lin, L. Y.; Wooley, K. L. *ACS Macro Lett.* **2012**, *1*, 328−333.
(59) Feher, F. J.; Wyndham, K. D.; Baldwin, R. K.; Soulivong, D.; Lichtenhan, J. D.; Ziller, J. W. *Chem. Commun.* **1999**, 1289−1290.
(60) Hua, C.; Peng, S.-M.; Dong, C.-M. *Macromolecules* **2008**, *41*, 6686−6695.
(61) Gunes, K.; Isayev, A. I.; Li, X. P.; Wesdemiotis, C. *Polymer* **2010**, *51*, 1071−1081.
(62) Chan, J. W.; Hoyle, C. E.; Lowe, A. B. *J. Am. Chem. Soc.* **2009**, *131*, 5751−5753.
(63) Konkolewicz, D.; Gray-Weale, A.; Perrier, S. B. *J. Am. Chem. Soc.* **2009**, *131*, 18075−18077.
(64) Zhang, W.; Müller, A. H. E. *Macromolecules* **2010**, *43*, 3148−3152.
(65) Gao, H.; Matyjaszewski, K. *Macromolecules* **2006**, *39*, 4960−4965.
(66) Vogt, A. P.; Sumerlin, B. S. *Macromolecules* **2006**, *39*, 5286−5292.
(67) Kim, B.-S.; Mather, P. T. *Macromolecules* **2006**, *39*, 9253−9260.
(68) Kim, B.-S.; Mather, P. T. *Polymer* **2006**, *47*, 6202−6207.
(69) Kim, B. S.; Mather, P. T. *Macromolecules* **2002**, *35*, 8378−8384.